Interrogation of "Surface," "Skin," and "Core" Orientation in Thermotropic Liquid-Crystalline Copolyester Moldings by Near-Edge X-Ray Absorption Fine Structure and Wide-Angle X-Ray Scattering

Stanley Rendon,[1] Robert A. Bubeck,[2] Lowell S. Thomas,[2] Wesley R. Burghardt,[1] Alexander Hexemer,[3] Daniel A. Fischer[4]

[1]*Department of Chemical and Biological Engineering, Northwestern University, Evanston, Illinois 60208*
[2]*Michigan Molecular Institute, Midland, Michigan 48640-2696*
[3]*Materials Research Lab, University of California at Santa Barbara, Santa Barbara, California 93106*
[4]*National Institute of Standards and Technology, 100 Bureau Drive, Stop-8523, Gaithersburg, Maryland 20899*

Received 7 February 2007; accepted 2 May 2007
DOI 10.1002/app.26759
Published online 27 July 2007 in Wiley InterScience (www.interscience.wiley.com).

ABSTRACT: Injection molding thermotropic liquid-crystalline polymers (TLCPs) usually results in the fabrication of molded articles that possess complex states of orientation that vary greatly as a function of thickness. "Skin-core" morphologies are often observed in TLCP moldings. Given that both "core" and "skin" orientation states may often differ both in magnitude and direction, deconvolution of these complex orientation states requires a method to separately characterize molecular orientation in the surface region. A combination of two-dimensional wide-angle X-ray scattering (WAXS) in transmission and near-edge X-ray absorption fine structure (NEXAFS) spectroscopy is used to probe the molecular orientation in injection molded plaques fabricated from a 4,4′-dihydroxy-α-methylstilbene (DHαMS)-based thermotropic liquid crystalline copolyester. Partial electron yield (PEY) mode NEXAFS is a noninvasive *ex situ* characterization tool with exquisite surface sensitivity that samples to a depth of 2 nm. The effects of plaque geometry and injection molding processing conditions on surface orientation in the regions on- and off- axis to the centerline of injection molded plaques are presented and discussed. Quantitative comparisons are made between orientation parameters obtained by NEXAFS and those from 2D WAXS in transmission, which are dominated by the microstructure in the skin and core regions. Some qualitative comparisons are also made with 2D WAXS results from the literature. © 2007 Wiley Periodicals, Inc. J Appl Polym Sci 106: 2502–2514, 2007

Key words: NEXAFS; liquid crystalline polymer (LCP); injection molding; orientation

INTRODUCTION

Thermotropic liquid crystalline polymers (TLCPs) have found a niche in commercial applications that require excellent processability, mold filling precision, physical properties, thermal stability, and dimensional stability. The ability to injection mold with ease is a direct result of the spontaneous ordering of molecules during flow. Despite considerable promise however, TLCPs have yet to find widespread use in applications that can exploit their potential as high strength/low weight engineering materials.[1] A severe processing issue is the frequent development of highly unidirectional molecular anisotropy, which limits the ability to sustain balanced macroscopic properties in many injection molded articles.[2] Directional processing methods such as injection molding often lead to skin-core morphologies on the surface and the interior, respectively, of the finished part.[3] Because processing of TLCPs involves a strong coupling between process conditions, flow-induced molecular orientation, and the resulting molecular-scale structure, understanding the factors that control the evolution of molecular orientation as a result of processing is a necessary prerequisite toward optimized fabrication of TLCP net-shaped molded parts.

The orientation of the skin layer in TLCP moldings is often difficult to deconvolute from that of the core when using wide-angle X-ray scattering (WAXS) data obtained in transmission. One laborious option described by Plummer et al.[4] and Dreher et al.[5] was to quantify skin orientation in TLCP moldings using WAXS of microtomed layers. Another method was to utilize attenuated reflection fourier transform

This material is based upon work supported by the National Science Foundation. Any opinions, findings, and conclusions or recommendations expressed in this material are those of the author(s) and do not necessarily reflect the views of the National Science Foundation.

Correspondence to: R. A. Bubeck (bubeck@mmi.org).

Contract grant sponsor: National Science Foundation; contract grant numbers: DMI-0132519, DMI-0521771, DMI-0521923.

infrared dichroism (ATR FTIR), although this technique is limited to a depth resolution of 5 μm.[6] A less invasive and more precise means of determining surface orientation directly presents itself in the form of NEXAFS spectroscopy.[7] NEXAFS is a synchrotron source soft X-ray spectroscopy technique that is sensitive to the orientation of phenyl groups via the intensity, I, of the partial electron yield (PEY) of Auger electrons of $1s \rightarrow \pi^*$ transition of the C=C bonds. A depth of just 2–3 nm can be selectively characterized using the PEY mode of the NEXAFS measurement whereas depths of ~100 nm can be probed using the fluorescence yield (FY) mode. The orientation is determined through a series of measurements of the carbon K edge spectrum over a range of incident angles, θ, of a monochromated linearly polarized beam relative to the sample surface. This technique has been successfully used to determine the orientation in LC alignment on rubbed polyimide substrates by Stöhr and Samant.[8] The formalisms behind this technique have been refined by Genzer et al.[9]

NEXAFS allows for the determination of a uniaxial orientation parameter, S, which may be computed from the analysis of $I(\theta)$, following techniques previously employed Stöhr and Samant.[8] Unlike other spectroscopic techniques that have been used to study surface orientation in TLCP moldings, this method can critically evaluate the symmetry of the orientation state, allowing characterization of *biaxial* orientation states (if present) of molecular orientation. A biaxial nematic is a type of nematic phase where chain molecules with anisotropic cross-sections are so organized in a mesophase that there is long range orientational order about all three orthogonal axes (i.e., rotation correlation about these axes).[1] Even a more conventional uniaxial nematic may exhibit a biaxial orientation state during flow, if flow-induced changes are able to perturb the molecular orientation distribution function away from its equilibrium uniaxial symmetry. To evaluate the symmetry of the orientation using NEXAFS, a molded sample is rotated about the axis in which it's oriented relative to the beam. A principal feature of the definition of orientation parameter of the Stöhr scheme is that S of the π^* transition dipole moment of the C=C bond segments is defined relative to the surface normal of the sample. Preliminary work on DHαMS moldings adopted this method for computing near surface skin order parameters for relatively thin plaques.[7] Work presented here however, adopts a new analysis scheme proposed (and demonstrated) by Pattison et al.[10] that defines S of the molecular axis, as related to the π^* transition dipole moment of the C=C bond segment in the direction of processing (surface rubbing direction in their case, melt flow direction in our case). This method results in determinations of S for molecular orientation parameters of aligned nematic polymers that are directly comparable with other techniques such as ATR-FTIR and WAXS. Here, we use NEXAFS and WAXS to compare the relative magnitude and direction of near surface, skin, and core molecular order parameters by characterization of injection molded plaques made from various molding processing conditions and geometries. A brief treatment and comparison of the Stöhr[8] versus the Kramer scheme, as presented in Pattison et al.,[10] is provided in the Appendix section.

EXPERIMENTAL

Materials and fabrication

The TLCP system utilized in this study was a precommercial copolyester containing 4,4′-dihydroxy-α-methylstilbene (DHαMS) as the mesogen and a 65/10/25 terephthalate/isophthalate/2,6-naphthalenedicarboxylate molar ratio.[11] The chemical structure for DHαMS is presented in Figure 1. Polymers with molecular weights of about 35,000 g/mol were evaluated.

Two types of sample plaques were fabricated using a Boy 30T2 injection molding machine with which molding parameters were controlled. Two types of insert molds were used, both of which were made by Master Precision Mold Technology, Inc. (Greenville, MI). The *Type I* plaque measures 76.2 mm × 76.2 mm and was molded with a coat hanger gate [Fig. 2(a)]. The *Type II* plaque measures 50.8 mm × 76.2 mm and was molded with a narrow port

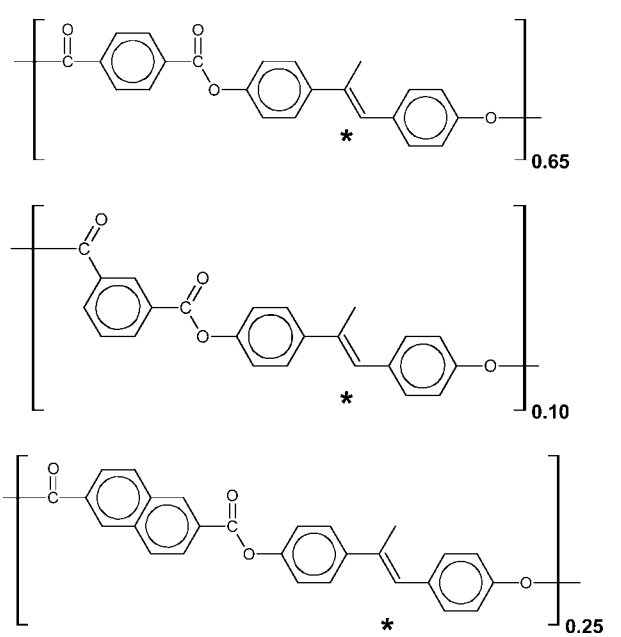

Figure 1 Chemical structure illustrating the principal components of the 4,4′-dihydroxy-α-methylstilbene (DHαMS)-based copolyester TLCP. The asterisk denotes the stilbene linkage.

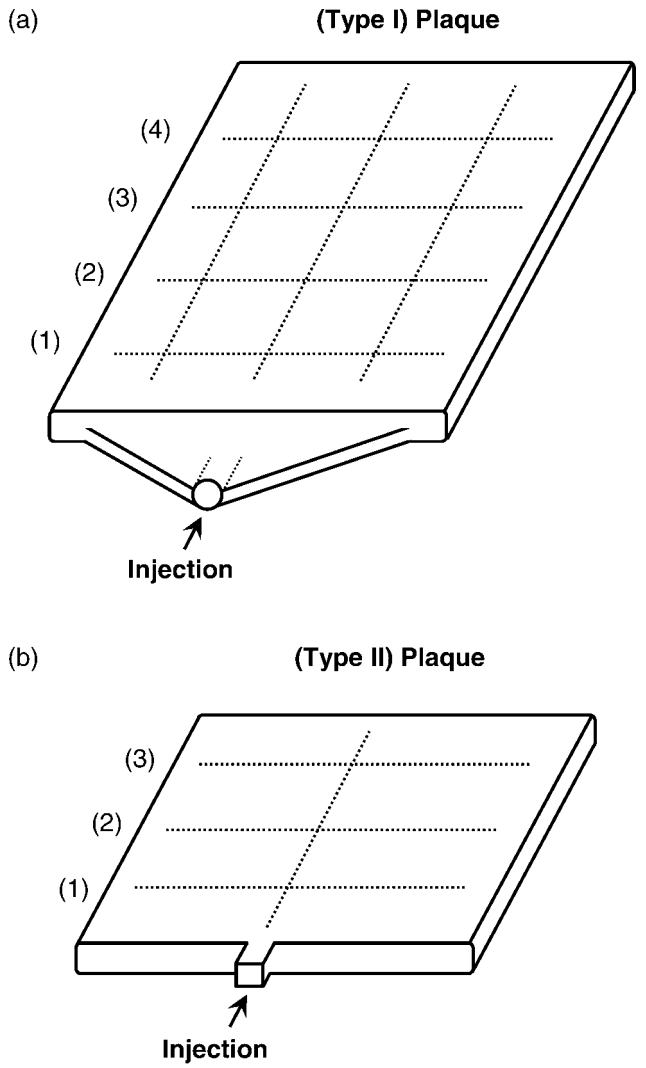

Figure 2 Injection molded plaque geometries used in WAXS and NEXAFS studies: (a) Type I plaques are 76.2 mm × 76.2 mm, and (b) Type II plaques measure 50.8 mm × 76.2 mm. The Type I plaque configuration features a coat hanger gate whereas the Type II configuration features a narrow gate. The arrow indicates the principal direction of flow. Dotted lines indicate the path locations where 2D WAXS measurements were performed (each numbered 15 mm apart).

gate midpoint on the longer side [Fig. 2(b)]. The narrow gate results in a more complex fill pattern than the coat hanger gate, which favors a more uniform flow pattern. The molds were fitted with inserts with polished faces that permitted the fabrication of plaques of various thicknesses. These were selected to be 0.8, 1.6, and 3.2 mm. Typically, the total cycle time was 47 s, the screw speed was 264 rpm, pack (holding) pressure was 280 bar (2.8×10^7 Pa), and the cooling (hold) time was 16 s. Injection fill times of 1 and 5 s were studied and these two times were obtained by varying the injection pressure alone to the two values of 1391 bar (1.39×10^8 Pa) and 140 bar (1.40×10^7 Pa), respectively. In addition to a range of melt temperatures, two mold temperatures (90 and 45°C) were studied.

Given that NEXAFS is a surface spectroscopy technique, knowledge of the surface topology of the plaques does prove useful. Prior to NEXAFS examination, it was ascertained that molded samples required surface cleaning to remove any contaminants. The cleaning was performed using a 1% solution of Alconox Liqui-Nox® cleaning agent (Alconox, White Plains, NY) in deionized water sonicated with a Bransonic 220 ultrasonic cleaner (Bransonic, Danbury, CT) for a duration of 10 min. Both the initial presence of contaminants and their effective removal were verified for a selected number of DHαMS copolyester plaque surfaces by atomic force microscopy (AFM) using a Topometrix 2000 AFM in oscillating mode. As shown previously,[7] AFM revealed two principal topological features on the plaque surfaces: a fine texture on the order of 1 nm in height and a much broader feature in the form of corrugations with low gradient slopes of the order of 8 nm in height and 200 nm in width at the base. The broad corrugations are aligned in the principal direction of flow. Neither feature was deemed likely to significantly interfere with the NEXAFS measurements.

2D WAXS and data analyses of injection molded plaques

Two-dimensional orientation maps were determined for each plaque type using WAXS measurements (in transmission mode) performed at 20 keV (0.62 Å) for multiple positions on the samples using the 5BM-D beamline of DND-CAT at the Advanced Photon Source of Argonne National Lab. An incident X-ray beam with a 1-mm-diameter size was used. A MarCCD detector was used to collect 512 × 512 pixel raw X-ray scattering patterns with 15-s exposures. WAXS patterns showed significant bimodal contributions from both the core and the skin obtained for 1.6 and 3.2 mm thick plaques. Previous work by Bubeck et al.[7] demonstrated that in relatively ''thin'' 0.8 mm thick plaques, uniaxial orientation is usually dominant along the centerline. Figure 3 provides representative WAXS patterns at a specific centerline location of a 0.8 mm thick [Fig. 3(a)] and 3.2 mm [Fig. 3(b)] thick Type I DHαMS plaque. Although part (a) shows strong unimodal orientation state, part (b) reveals the presence of bimodal diffraction peaks with equatorial scattering reflecting orientation induced by shear flow at the mold surfaces and meridional scattering indicating transverse extensional character.[12]

The term ''skin'' layer describes a very specific morphological region within the thickness layer of molded articles. In the context of this work, we asso-

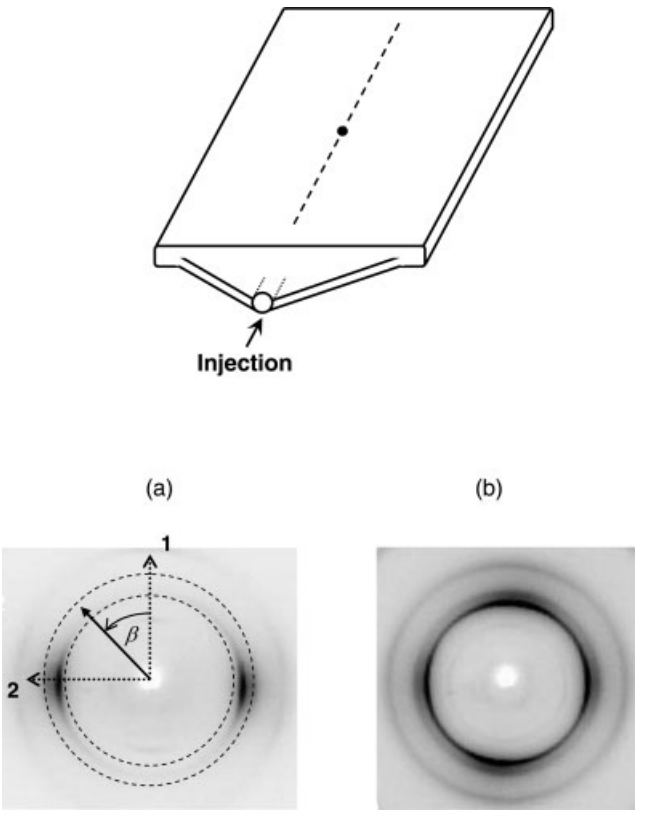

Figure 3 Physical orientation of a Type I injection molded plaque along with two representative 2D WAXS patterns taken for a centerline position of a: (a) 0.8 mm thick molded plaque showing unimodal orientation state due to dominance of shear flow and a (b) 3.2 mm thick plaque showing bimodal orientation populations reflecting competition between shear and extension. Plaques were processed at constant fast fill time with melt and mold temperatures of 270 and 45°C, respectively. The overlays in (a) define the coordinates and range of the scattering wave vector, q, used for the extraction of azimuthal scans; β is the azimuthal angle measured away from the vertical filling direction.

ciate the skin region with two distinct levels of morphology: (1) a high alignment right at the outer most surface, associated with fountain-flow and rapid solidification, and (2) a thicker ''shear-dominated'' region near the surface, distinct from transverse orientation in the core. This region has been observed previously in isothermal TLCP melt channel flows[12] and is distinct from traditional viewpoints of the definition of skin.[3,4] Figure 4 provides a schematic representation of a molded plaque depicting the near surface, skin, and core morphologies typically found along the thickness of LCP moldings. From this depiction it is clear that the skin encompasses both the layers of ''thin'' superficial high alignment near the surface as well as the ''thicker'' shear-dominated region present over a much broader depth through the thickness of the sample.

Quantitative determination of the ''skin'' and ''core'' regions of molecular orientation in molded plaques involved computing order parameters from azimuthal intensity scans extracted from 2D WAXS patterns collected in transmission. Because 1D azimuthal scans contain information averaged through the entire plaque thickness (Fig. 4), ''skin'' and ''core'' contributions to the orientation must be computed separately. As previously described by Rendon et al.[12] and Bubeck et al.,[7] bimodal azimuthal scans typically have two different sets of intensity peaks that are attributed to the strength and direction of skin (driven by shear flow) and core (driven by transverse extension) orientational contributions. To isolate each set of peaks we utilize an appropriate deconvolution technique (provided an appropriate baseline is used) that generates two separate azimuthal scans describing the distribution of orientation over two different depths in the sample (Fig. 5). Since the shape of azimuthal scans is generally Gaussian-like, it is possible to isolate each set of intensity peaks from a ''bulk'' azimuthal scan via a Gaussian deconvolution method (using Peakfit®). Having done this, we next assume uniaxial orientation within either population to compute the corresponding order parameters based on the usual Herman's convention:[13]

$$S = \frac{1}{2}(3\cos^2\beta - 1) \tag{1}$$

where in the limit of perfect orientation, independent of direction, this quantity will yield a value of 1, whereas 0 reflects a randomized orientation state (i.e., isotropic). Although the assumption of uniaxial symmetry is perhaps not fully appropriate in this case, it presents a vast improvement over any calculations involving the full $I(\beta)$ from the bulk azi-

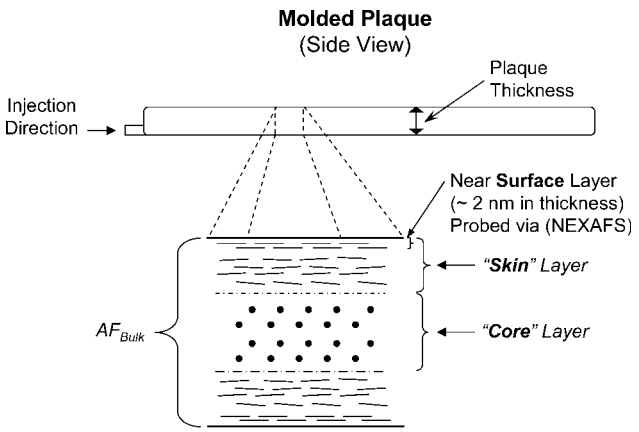

Figure 4 Idealized representation of an injection molded plaque cross-section illustrating the various levels of morphology present along the plaque thickness direction. 2D WAXS in transmission averages structural information through the sample thickness while NEXAFS probes molecular orientation over depths of 2–3 nm in the near surface layer.

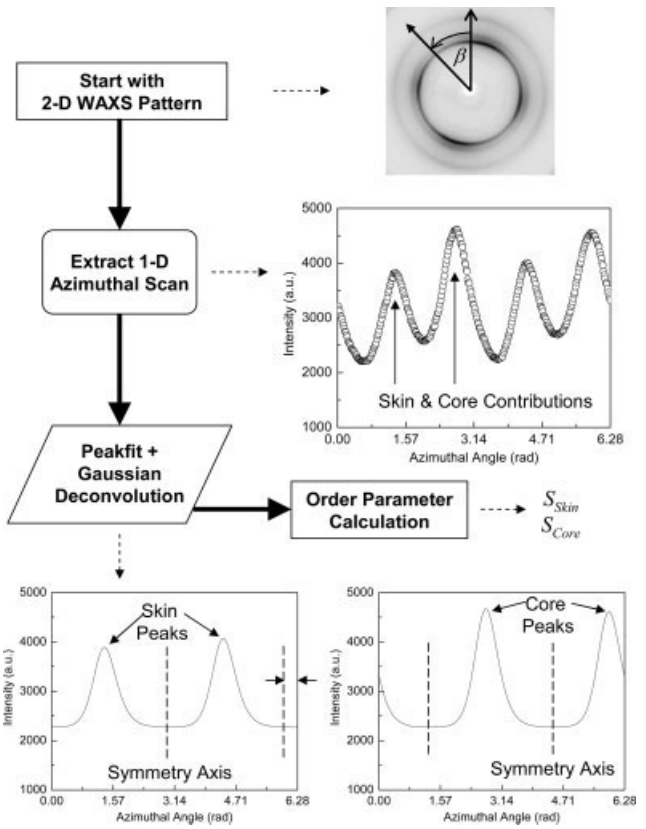

Figure 5 Data analysis procedure used to extract azimuthal intensity scans describing the scattering contributions due to shear (''skin'') and extension (''core''). Two $I(\beta)$ scans are extracted from a single 1D ''bulk'' sample azimuthal scan via a Gaussian deconvolution of azimuthal intensity peaks. Resulting scans are subsequently processed to compute S_{Skin} and S_{Core}.

muthal scan. Here, Herman's order parameters that reflect the *skin* layer contribution to the bulk molecular orientation (S_{Skin}) are computed from 1D azimuthal intensity scans that only contain peak intensity information from orientational contributions due to *shear flow* (Fig. 5). Similarly, localized *core* contributions to the bulk molecular orientation (S_{Core}) are computed from azimuthal scans which only contain peak intensity information due to transverse extension. In computing these order parameters, it is necessary to redefine the azimuthal angle, β, to start at the symmetry axis for each separate population of orientation as presented in Figure 5. These order parameters are computed using a Matlab® script, which takes the azimuthally integrated dataset and splits it into four equal segments, whose minimum intensity occurs at zero radians and whose maximum intensity occurs at $\pi/2$. The program then computes the order parameters for each of the four regions following the technique by Mitchell and Windle.[14] This simply involves computing the second Legendre polynomial (P_{2n}), which can be correlated to the order parameter. The output gives four values of S along with the average of the four. Background scattering is accounted for in the computation of the order parameter by using a baseline value of the azimuthal intensity (which eliminates any parasitic scattering). This baseline is computed for the pattern with the highest anisotropy and corresponding lowest intensity. This value of intensity is then subtracted from all of the other frames in the dataset. Final corrected values of the order parameter (either S_{Skin} or S_{Core}) are then compared with the values of surface molecular orientation obtained by NEXAFS.

In this study, we also present 2D vector plots to describe the distribution of bulk molecular orientation in several TLCP plaques. For these data we have used a second moment tensor analysis scheme previously described by Rendon et al.[12] to characterize the degree and direction of through-thickness molecular orientation in moldings. The degree of orientation is denoted by ''Anisotropy Factor'' or AF, which, like the Herman's orientation function, ranges between 0 for an isotropic state and 1 for perfect orientation; however, this analysis requires no assumption about the symmetry of the orientation distribution function and is hence more appropriate for analysis of the full azimuthal intensity scans.

NEXAFS experimental setup and data analysis

NEXAFS experiments were performed on the NIST/Dow soft X-ray materials characterization facility (beamline U7A) at the National Synchrotron Light Source at Brookhaven National Laboratory. The capabilities of this beamline have been described by Genzer et al.[15] The beamline soft X-rays had a degree of polarization of about 85% and an incident energy photon resolution and approximate intensity of 0.1 eV and 5×10^{10} photons/s, respectively. The NEXAFS partial electron yield (PEY) signal was collected using a channeltron electron multiplier fitted with an electrostatic three grid high pass electron kinetic energy filter. A grid bias of −150 V was used.

The orientation of the copolyester polymer molecules in the near surface region (upper 2 nm) was examined using the PEY signals obtained as described above. Details of the technique as applied to semifluorinated polymers appear elsewhere.[15–17] The PEY spectra for the carbon K edge were obtained for each sample over the incident angles relative to the sample surface of 20°, 30°, 40°, 55°, 60°, 70°, 80°, and 90°, normalized in the energy range of 280–315 eV, and the relative intensities, $I(\theta)$, for the $1s \rightarrow \pi^*$ peak for the C=C bonds were recorded.

The expression for PEY $I(\theta)$ is predicted to take the form:

$$I(\theta) = A + B\sin^2\theta \quad (2)$$

regardless of the degree of orientation. A and B are coefficients from the linear equation describing the angular dependence of the intensity, I, where θ is the incident angle of the polarized beam. The near surface *molecular* orientation, S_{Surface}, based upon the Kramer scheme described by Pattison et al.[10] can be calculated using the expression:

$$S_{\text{Surface}} = \left(1 - \frac{2(A+B)}{A + \frac{B}{6P}(3P-1)}\right) \quad (3)$$

where P is the polarization factor of the elliptically polarized beam (0.85 for experiments reported here). Values for S using data obtained over the 30° to 80° incident angle range were reported to minimize any secondary effects that may be incurred from surface roughness and/or instrumental anomalies. It was over this more constricted incident angle range that the most linear behavior with the best confidence limits for the slope B was observed. The confidence limits for S derived from both WAXS and NEXAFS was ± 0.02. The variation in S_{Surface} as a function of azimuthal rotation angle for selected positions displaced from the centerline was determined by taking samples cut from the vicinity of the position, mounting them upon a sample manipulation bar inserted in the NEXAFS chamber, and individually rotating each to a specified angle, ϕ, for each set of PEY scans taken.

The three determinations of molecular orientation, S, presented in Table I, effectively give measures of their magnitude and direction at three levels of depth from the surface: S_{Surface} yields near surface orientation to a depth of 2–3 nm; S_{Skin} describes ''in-shear'' molecular orientation resulting from contributions due to the ''skin'' region (~0.4 mm). As stated earlier, the term ''skin'' encompasses both the layers of ''thin'' superficial high alignment near the surface (described by S_{Surface}) as well as the ''thicker'' shear-dominated region present over a much broader depth through the thickness of the sample. Finally, S_{Core} indicates molecular orientation, if existent, for the remaining ''core'' thickness for the 1.6 and 3.2 mm thick plaques. Values for AF_{Bulk} indicate the average bulk (or through-thickness) orientation for a given position based on the second moment tensor analysis method described elsewhere.[12]

RESULTS AND DISCUSSION

Surface orientation via NEXAFS

An example of a set of NEXAFS carbon K edge spectra for the surface skin of an injection molded plaque is shown in Figure 6. The spectra were measured as a function of incident angle of the beam relative to the sample surface. The sample was cut from the middle of the sample close to the vent end edge of a plaque [position ''4'' in Fig. 2(a)] molded with a melt temperature of 290°C and a mold temperature of 45°C. The π^* $(C{=}C)_1$ peaks from the in-plane C=C bonds are minimized when the polarized beam is perpendicular to the surface (θ = 90°) and the complementary σ orbital peaks are correspondingly maximized. This result is consistent with molecular alignment in the plane of the plaque skin and the corresponding π orbital for the C=C bonds being perpendicular to the sample surface. The intensity of the π^* $(C{=}C)_1$ peak varies linearly with $\sin^2$ of the incident angle, θ, as per eq. (2), an exam-

TABLE I
Summary of Molding Conditions and Resulting Orientation Parameters Obtained at ''Off-Axis'' Locations in Type I and Type II Molded Plaques

Plaque type	Thickness (mm)	T_{melt} (°C)	T_{mold} (°C)	Fill rate (s)	S_{Surface}[a]	S_{Skin}[b]	S_{Core}[c]	$\phi_{\text{max (deg)}}$[d]	$\beta_{\text{max (deg)}}$[e]	AF_{Bulk}[f]
I	1.6	290	45	1	0.80	0.55	0.24	25	20	0.37
I	1.6	270	45	1	0.76	0.48	0.17	15	10	0.43
I	0.8	270	45	1	0.76	0.66	N/A	19	15	0.68
I	3.2	270	45	1	0.74	0.22	0.28	13	8	0.10
I	3.2	290	90	5	0.71	0.50	0.24	7	2	0.45
I	3.2	245	90	5	0.71	0.29	0.27	20	14	0.21
II	3.2	245	45	1	0.76	0.24	0.57	41	35	0.37
II	3.2	290	45	1	0.73	0.23	0.25	49	40	0.19

[a] Near surface molecular order parameter obtained by NEXAFS computed using eqs. (2) and (3).
[b] Order parameter obtained by WAXS describing the skin contribution to the orientation.
[c] Order parameter obtained by WAXS describing the core contribution to the orientation.
[d] Azimuthal sample rotation angle associated with the maximum surface molecular orientation.
[e] Azimuthal angle indicative of the average orientation direction in the skin region as determined by WAXS.
[f] Anisotropy factor for the bulk through-thickness sample computed using the second moment tensor analysis described by Rendon et al.[12]

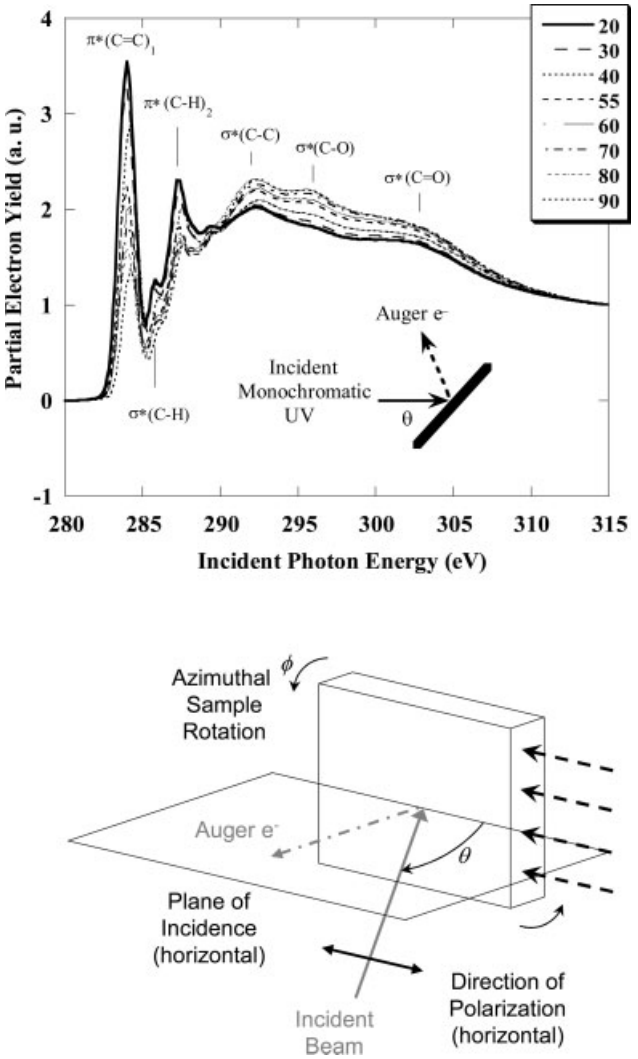

Figure 6 Representative NEXAFS Carbon K edge spectra for a DHαMS copolyester plaque surface. Spectra collected at varying angle of incident beam relative to the surface. Beam polarization is aligned with the direction of maximum orientation. Process parameters: melt temperature = 290°C, mold temperature = 45°C.

ple of which is shown in Figure 7. Determination of the order parameter $S_{Surface}$ was accomplished using eqs. (2) and (3). The nearly flat slope for the case of orientation perpendicular to the flow direction indicates that the surface orientation is almost completely uniaxial (i.e., very limited biaxiality) in the area examined. This general result is identical to that observed by Stöhr and Samant[8] for aligned polyimides and liquid crystals containing phenyl groups in their molecular backbones with cylindrical symmetry about the long axis (i.e., uniaxial nematic) and the π orbitals perpendicular to the long axis.

Order parameters derived from the NEXAFS analyses along the centerline of molded plaques studied here ranged from about 0.71–0.80 depending on position and processing conditions and always with the flow direction in the plane of incidence of X-ray beam. The following discussion of results proceeds from relatively simple cases of flow-induced surface orientation along sample centerlines in plaques that are coat hanger gated to the more complex cases involving orientation states away from the centerline and with a narrow gate.

Effect of processing conditions on Type I plaques

Type I plaques presented in this work were fabricated using a tool fitted with a ''coat hanger'' gate, which permits a relatively even flow of polymer into the mold. This particular configuration was chosen to study less complex filling conditions and also to provide a source of plaques from which tensile samples with relatively simple orientation states could be machined and mechanically characterized. Mechanical and morphological anisotropy data for these plaques are presented elsewhere.[18]

The effect of mold temperature on the centerline surface orientation of a Type I molded plaque is shown in Figures 8 and 9 for two melt temperatures. At a melt temperature of 290°C, $S_{Surface}$ ranges from about 10–20% more for a 45°C mold temperature than for a 90°C mold temperature (Fig. 8). This result is consistent with the notion that rapid cooling and crystallization derived from the colder mold will yield thinner surface layer within the skin having enhanced orientation along the shear direction. If a more unusual melt temperature of 245°C is chosen, then the relative orientations obtained for the same two mold temperatures reverse their ranking for retained surface orientation (Fig. 9). The higher mold

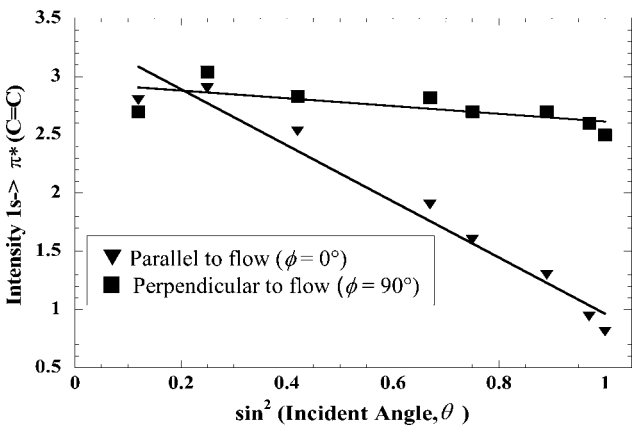

Figure 7 Analysis of C=C π* absorption intensity dependence on incident angle, from which molecular order parameter in surface region may be extracted. Angular dependence of resonance is shown parallel and perpendicular to the principal direction of shear flow at the surface of an injection molded DHαMS plaque. Beam polarization was aligned parallel to the principal flow direction and then perpendicular to the principal flow direction to obtain the two sets of data.

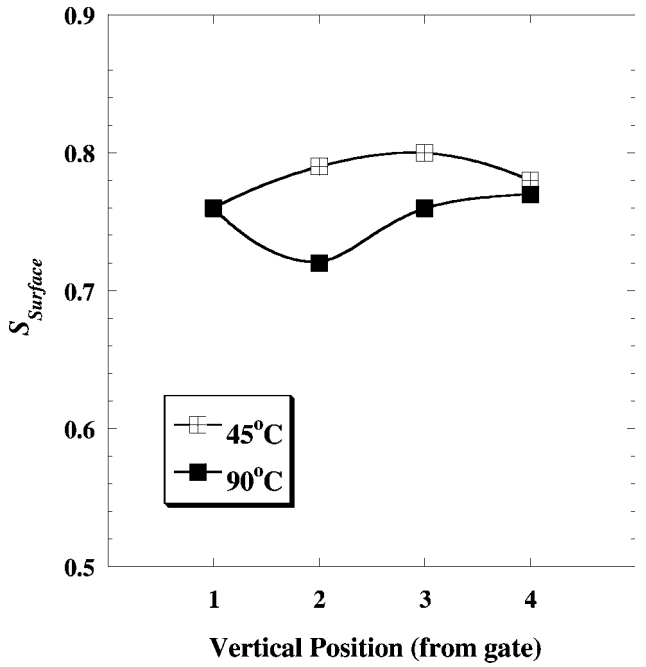

Figure 8 A comparison of molecular order parameters ($S_{Surface}$) derived from the NEXAFS method for two mold temperatures (45 and 90°C) as a function of vertical position from the gate along the centerline of two 1.6 mm thick injection molded Type I DHαMS plaques. The numbered positions correspond to those indicated in Figure 2(a). Constant processing conditions: melt temperature = 290°C and fast fill.

temperature is required to obtain relatively uniform orientation for the four plaque positions, particularly on the gated end (Position ''1''). The competing effects of mold and melt temperature processing conditions on near surface orientation shown in Figures 8 and 9, indicate a reversal of surface orientation for mold temperatures of 45 and 90°C for melt temperatures of 245 and 290°C. A possible explanation for these results is that at 245°C (the extreme lower edge of the melting range) greater orientation is obtained by permitting more shear flow before solidification with the 90°C mold temperature, whereas at 290°C (the point of maximum endothermic melting behavior) greater orientation is retained by the more rapid crystallization induced by the colder 45°C mold.

Results obtained at an off-axis position (equidistant between the gate and vent edges and the centerline and the side edge) for two representative Type I plaques are presented in Figures 10 and 11. Each figure shows a 2D WAXS pattern at the measurement location, a vector map of the average bulk orientation distribution derived from such WAXS data, and a plot of the slope, $-B$, given by eq. (2) as a function of azimuthal sample rotation angle, ϕ, derived from multiple NEXAFS measurements taken at the position indicated on the vector plot. Based on centerline results (Fig. 7); we expect that the maximum slope corresponds to the sample orientation in which the surface orientation direction coincides with the plane of incidence. This, then, provides a way to identify the surface orientation direction. Once aligned at this direction, eq. (3) may be used to extract $S_{Surface}$. The direction of maximum surface orientation, ϕ_{max}, determined via NEXAFS, is used to interpolate between known values of $S_{Surface}$, which allows for subsequent calculation of the corresponding maximum surface order parameter. Arrows in the WAXS patterns indicate scattering contributions due to ''skin'' shearing kinematics and midplane extension in the ''core'' associated with melt flow. The processing conditions, plaque types and thicknesses, and values of corresponding values of S, as determined by WAXS and NEXAFS, are summarized in Table I for all plaques studied at off-axis locations.

The results illustrated in Figures 10 and 11 are for nearly identical processing conditions (45°C mold temperature, 1.6 mm plaque thickness, and 1 s fill time), the only difference being the melt temperature (290 vs. 270°C). The principal loss of orientation associated with the 20°C decrease in melt temperature was realized in the core where extensional flow dominates. Corresponding decreases in mechanical properties in the direction of maximum orientation have also been observed with decrease in melt tem-

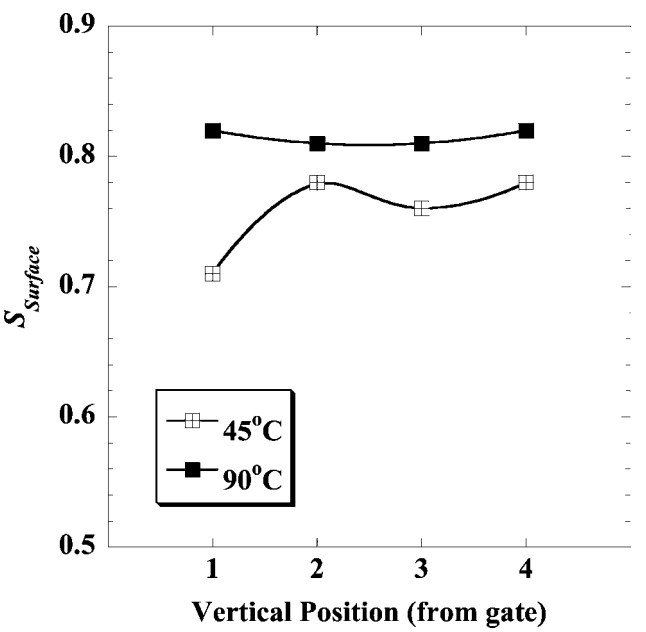

Figure 9 A comparison of molecular order parameters ($S_{Surface}$) derived from the NEXAFS method for two mold temperatures (45 and 90°C) as a function of vertical position from the gate along the centerline of two 1.6 mm thick injection molded Type I DHαMS plaques. The numbered positions correspond to those indicated in Figure 2(a). Constant processing conditions: melt temperature = 245°C and fast fill.

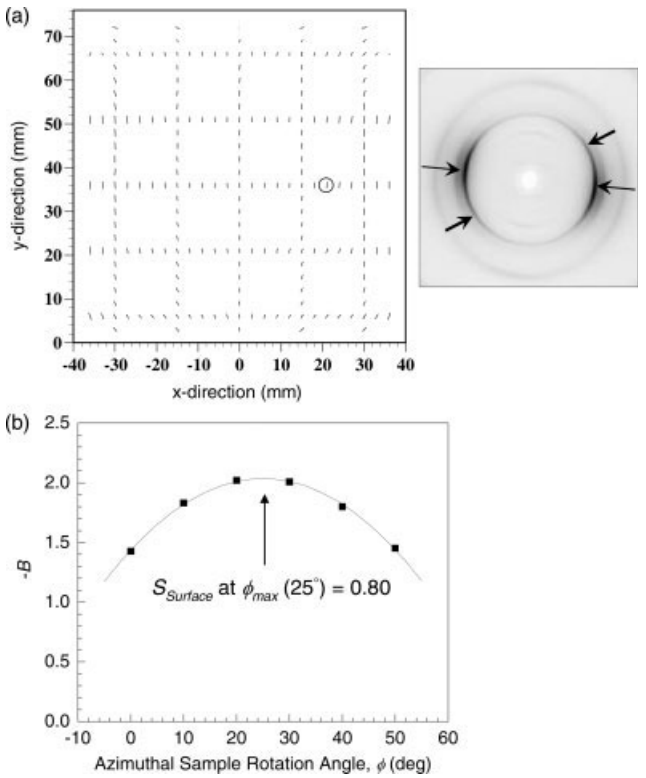

Figure 10 WAXS and NEXAFS characterization of a 1.6 mm thick Type I DHαMS plaque. (a) Vector plot representation of molecular orientation using the second moment tensor description of anisotropy factor and average orientation direction described by Rendon et al.[12] X-ray pattern collected at the specified sample position (on vector plot) where WAXS and NEXAFS measurements were performed. Coat hanger entry gate is located at coordinate position $x = 0$ mm and $y = 0$ mm. Thin arrows in the X-ray pattern indicate scattering contribution due to ''skin'' shearing kinematics and heavy arrows indicate scattering contribution due to mid-plane extension in the ''core.'' (b) Plot of the slope from $I(\theta)$ given in eq. (2) versus azimuthal rotation angle, ϕ. Maximum surface orientation ($S_{surface} = 0.80$) found at $\phi_{max} = 25°$. Sample was extracted from a plaque processed at 1 s fill time with melt and mold temperatures of 290 and 45°C, respectively.

perature.[18] The maximum molecular orientation on the near surface decreased slightly ($S_{Surface} = 0.80$ vs. 0.76) with a decrease in melt temperature whereas the order parameter associated with shear flow contributions to the orientation was more greatly affected ($S_{Skin} = 0.55$ vs. 0.48), reflecting the fact that the WAXS probes more deeply into the sample than does NEXAFS (see Table I).

Halving the plaque thickness to 0.8 mm with the same melt processing temperature of 270°C resulted in an overall increase in S_{Skin} from 0.48 to 0.66, but no change in the molecular order parameter at the near surface, $S_{Surface} = 0.76$. We postulate that the orientation in the core (S_{Core}) became, in essence, one with the skin (S_{Skin}) because the filling flow in general at this thickness is dominated by shear kinematics. At first glance, direct comparison of the near surface molecular orientation value between the 0.8 mm thick ($S_{Surface} = 0.76$) and the 1.6 mm thick ($S_{Surface} = 0.80$) plaques shown in Table I could suggest some disparity in the NEXAFS results. Closer inspection, however, does suggest that the higher melt temperature (290°C) of the thicker 1.6 mm plaque is the injection process parameter that is significantly responsible for the higher $S_{Surface}$ value when compared with that of the 0.8 mm thick plaque. It is plausible that the higher melt injection temperature lead to enhanced molecular orientation along the nominal flow direction even with the thicker plaque geometry. Doubling the plaque thickness from 1.6 to 3.2 mm at this melt temperature resulted in a loss of molecular orientation of the skin, but with much less

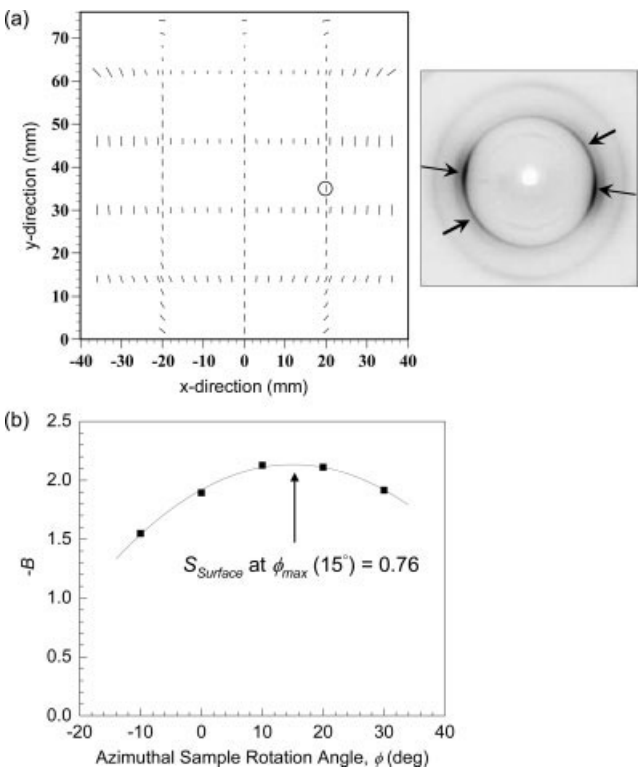

Figure 11 WAXS and NEXAFS characterization of a 1.6 mm thick Type I DHαMS plaque. (a) Vector plot representation of molecular orientation using the second moment tensor description of anisotropy factor and average orientation direction described by Rendon et al.[12] X-ray pattern collected at the specified sample position (on vector plot) where WAXS and NEXAFS measurements were performed. Coat hanger entry gate is located at coordinate position $x = 0$ mm and $y = 0$ mm. Thin arrows in the X-ray pattern indicate scattering contribution due to ''skin'' shearing kinematics and heavy arrows indicate scattering contribution due to mid-plane extension in the ''core.'' (b) Plot of the slope from $I(\theta)$ given in eq. (2) versus azimuthal rotation angle, ϕ. Maximum surface orientation ($S_{surface} = 0.76$) found at $\phi_{max} = 15°$. Sample was extracted from a plaque processed at 1 s fill time with melt and mold temperatures of 270 and 45°C, respectively.

influence on the near surface orientation. X-ray scattering patterns clearly reveal the predominance of bimodal populations of orientation. Shear flow has much less influence for the thicker mold, and time for cooling to the point of crystallization is longer, which both mitigate against maximizing orientation. This is especially clear in the value of the anisotropy factor (AF_{Bulk} = 0.10), which suggests very strong competition between shear and transverse extension leading to a significant reduction in the average orientation.

Within the range of melt temperatures between 245 and 290°C, the angle of maximum surface orientation remained fairly consistent (ϕ_{max} = 7–25°) overall all thicknesses. Some degree of error in these values is certainly reasonable given that each sample was rotated manually over increments of 10° prior to any measurements. Molecular orientation of the near surface ($S_{Surface}$) varied far less than the changes in orientation associated with S_{Skin} and particularly S_{Core}. This result is most likely associated with the fact that the material at the mold surface is the first to crystallize. The direction of maximum orientation, as indicated by the azimuthal rotation angle, ϕ, always coincided well for $S_{Surface}$ and S_{Skin} for the Type I plaques. The range of $S_{Surface}$ with change in azimuthal rotation angle of 50° for the Type I plaques never varied by more than about 10%, which is most likely a manifestation of the relatively even flow in the studied position of the mold with coat hanger gating.

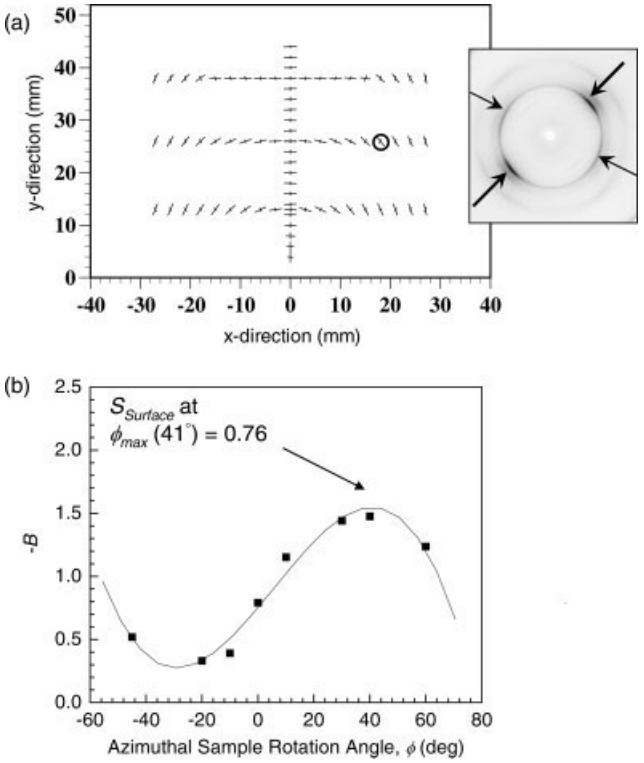

Figure 12 WAXS and NEXAFS characterization of a 3.2 mm thick Type II DHαMS plaque. (a) Vector plot representation of molecular orientation using the second moment tensor description of anisotropy factor and average orientation direction described by Rendon et al.[12] X-ray pattern collected at the specified sample position (on vector plot) where WAXS and NEXAFS measurements were performed. Entry gate is located at coordinate position x = 0 mm and y = 0 mm. Thin arrows in the X-ray pattern indicate scattering contribution due to ''skin'' shearing kinematics and heavy arrows indicate scattering contribution due to midplane extension in the ''core.'' (b) Plot of the slope from $I(\theta)$ given in eq. (2) versus azimuthal rotation angle, ϕ. Maximum surface orientation ($S_{surface}$ = 0.76) found at ϕ_{max} = 41°. Sample was extracted from a plaque processed at 1 s fill time with melt and mold temperatures of 245 and 45°C, respectively.

Effect of processing conditions on Type II plaques

The Type II plaques are 76.2 mm wide × 50.8 mm long plaques injection-molded with a tool fitted with a narrow gate positioned midpoint on the entry side [Fig. 2(b)]. This configuration was chosen in order to provide a filling condition that is more complex than that of the coat hanger gated Type I plaque configuration. The plaques were studied at their midpoint position off of the centerline, as shown in Figures 12 and 13. The results are for nearly identical processing conditions (45°C mold temperature, 3.2 mm plaque thickness, and 1 s fill time), the only difference being the melt temperature: 245 versus 290°C, respectively.

The direction of the maximum for $S_{Surface}$ in these Type II plaques coincides well for both melt processing temperature conditions. The values for molecular orientation at the near surface ($S_{Surface}$) are consistently about three times greater than those for S_{Skin}, as presented in Table I. This is consistent with the fact that WAXS probes through the plaque thickness whereas NEXAFS only provides a near surface description of the orientation that is dominated mostly by shearing kinematics. Although a lower melt temperature favored lower values of S_{Core} in the Type I plaques, the tendency is reversed for Type II. Spatially-varying competition between inhomogeneous mixed shear and transverse extension is known to lead to complex bimodal character based on expectations from prior isothermal channel flow studies on DHαMS and other commercial TLCPs.[18,19] As one might expect, the narrow gate results in a much less uniform set of orientation states than does the ''coat hanger'' gate. The range of values for molecular orientation parameters reported here are also similar in kind and magnitude to those reported by Pirnia and Sung[6] using the surface-specific technique of Fourier transform Infrared (FTIR) attenuated total reflection (ATR) dichroism. The sampling depth for the IR technique is about 5 μm, whereas PEY mode

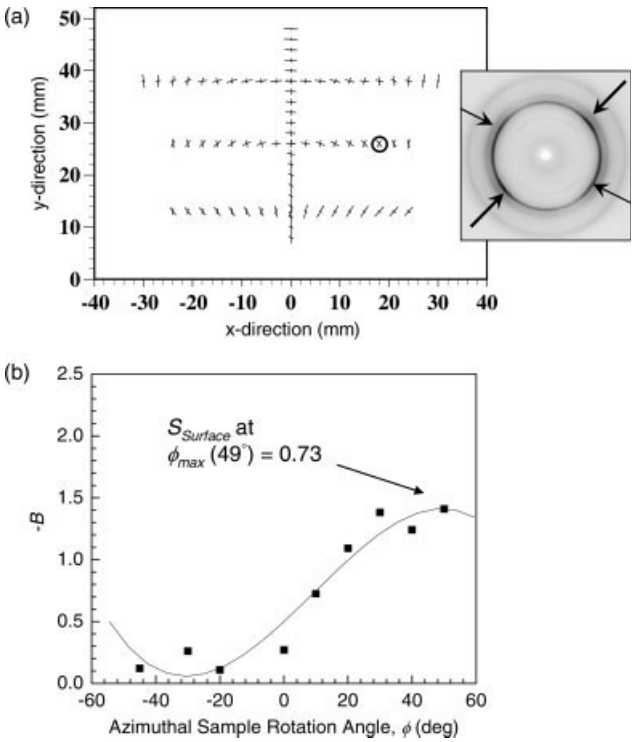

Figure 13 WAXS and NEXAFS characterization of a 3.2 mm thick Type II DHαMS plaque. (a) Vector plot representation of molecular orientation using the second moment tensor description of anisotropy factor and average orientation direction described by Rendon et al.[12] X-ray pattern collected at the specified sample position (on vector plot) where WAXS and NEXAFS measurements were performed. Entry gate is located at coordinate position $x = 0$ mm and $y = 0$ mm. Thin arrows in the X-ray pattern indicate scattering contribution due to ''skin'' shearing kinematics and heavy arrows indicate scattering contribution due to mid-plane extension in the ''core.'' (b) Plot of the slope from $I(\theta)$ given in eq. (2) versus azimuthal rotation angle, ϕ. Maximum surface orientation ($S_{surface} = 0.73$) found at $\phi_{max} = 49°$. Sample was extracted from a plaque processed at 1 s fill time with melt and mold temperatures of 290 and 45°C, respectively.

NEXAFS samples to a depth of 2 nm. We have obtained similar results in kind by a very similar ATR FTIR method based upon the use of a Herrick ''Seagull'' stage on samples for which 2D WAXS and NEXAFS data have also been obtained. As one might expect, the values of S obtained by IR are close but typically about 5% less than by NEXAFS. Future studies should entail characterizations of the state of orientation in these Type II plaques using a 6-axis sample manipulator stage for positions distanced from the centerline. The data in Figures 12 and 13 clearly show a distinct sigmoidal-type plot for $-B$ versus azimuthal sample rotation angle that differs from that of Type I plaques indicative of the more complex fill geometry for the Type II plaque compared to that for the Type I. The ability to rotate the sample azimuthally via a manipulator stage should enable more efficient and precise determination of surface orientation in the regions of high complexity of orientation compared to manual rotation of the samples as performed here.

CONCLUSIONS

The contributions of shear and extensional flows on the bimodal character of molecular orientation in the moldings have been characterized by a combination of NEXAFS spectroscopy and 2D WAXS in transmission. NEXAFS and WAXS have been used to characterize the orientation in injection molded plaques fabricated from thermotropic DHαMS copolyester. NEXAFS has been presented as a noninvasive *ex situ* means of determining surface layer orientation that samples to a depth as shallow as 2 nm and does not require slicing or ultramicrotoming of the samples to isolate the surface layers for interrogation. This method provides a complementary characterization tool, with exquisite surface sensitivity, to complement X-ray scattering methods which average orientation through the bulk sample thickness. The equivalency (or lack thereof) of orientation parameters obtained by using the WAXS in transmission and NEXAFS techniques has been verified for various molded plaque thicknesses and geometries. WAXS-based values of the skin (S_{Skin}) and core (S_{Core}) orientation parameters were always found to be lower in magnitude relative to NEXAFS-based near surface molecular order parameters over the full range of processing conditions and thicknesses studied. Overall, we suspect that the molecular orientation of the surface layer of the ''skin'' of the moldings examined by NEXAFS defines a region of ''thin'' very high alignment near the plaque surface as well as the ''thicker'' shear-dominated region present over a much broader depth through the thickness of the sample.

The NEXAFS experiments were carried out at the NIST/Dow soft X-ray materials characterization facility at the National Synchrotron Light Source, Brookhaven National Laboratory, which is supported by the United States Department of Energy, Division of Materials Sciences and Chemical Sciences. Wide-angle X-ray scattering experiments were conducted at the DuPont-Northwestern-Dow Collaborative Access Team (DND-CAT) Synchrotron Research Center located at Sector 5 of the Advanced Photon Source of Argonne National Laboratory. DND-CAT is supported by the E.I. DuPont de Nemours & Co., the Dow Chemical Company, and the National Science Foundation through Grant DMR-9304725 and the State of Illinois through the Department of Commerce and the Board of Higher Education Grant IBHE HECA NWU 96. Use of the Advanced Photon Source was supported by the U.S. Department of

Energy, Basic Energy Sciences, Office of Energy Research, under Contract No. W-31-102-Eng-38. The authors thank Edward J. Kramer (U. C. Santa Barbara), Xuefa Li, Sitaraman Krishnan, Christopher K. Ober (Cornell University), and Jun Fang (Northwestern University) for their collaboration during various stages of the project. The assistance of Mathew Stephenson (M.M.I.) in obtaining the AFM data and Judy Eastland (M.M.I.) for library support is greatly appreciated. Certain commercial equipment is identified in the article in order to adequately specify the experimental procedure. In no case does such identification imply recommendation or endorsement by the National Institute of Standards and Technology, nor does it imply that the items identified are necessarily the best available for the purpose.

APPENDIX: A BRIEF COMPARISON OF THE STÖHR AND KRAMER SCHEMES FOR NEXAFS DATA ANALYSES TO DETERMINE MOLECULAR SURFACE ORIENTATION

The convention that has usually been adopted to extract orientation parameters from variable incident angle NEXAFS data of the carbon K edge is the method of Stöhr and Samant.[8] This convention is based upon a configuration in which the perpendicular relationship for the coordinates of the analysis is taken relative to the normal to the sample surface. This convention has been used by several authors,[15–17,20] including previous work on the surface orientation in TLCPs.[7] Under this convention, an average uniaxial orientation parameter, S_a, is defined as:

$$S_a = \frac{1}{2}(3f_z - 1) \tag{A.1}$$

where f_z is one of the three molecular orientation factors (along with f_x and f_y, where $f_x + f_y + f_z = 1$), with z being the axis normal to the sample surface. If one uses the method of Stöhr and Samant[8] to determine an average orientation, S_a, parallel to the sample surface, we arrive at the expression:

$$S_a = \frac{-P^{-1}B}{[3A + (3 - P^{-1})B]} \tag{A.2}$$

where P is the polarization factor of the elliptically polarized beam (0.85 for experiments reported here).

The order parameter S_M of the main molecular main-chain axis in the principal direction of flow in an x-axis direction in the sample surface can alternatively be defined for when the molecular axis is oriented at an angle α from the x-axis. The transition dipole moment of the π^* orbitals are oriented at an angle (90°, α) relative to the x-axis. The orientation factor f_x now represents the projection of the transition dipole moment of the π^* orbitals onto the x-axis; consequently $f_x = 1 - \cos^2\alpha$. From this definition, Kramer arrives at an expression for S_M, as reported by Pattison et al.,[10]

$$S_M = \frac{1}{2}(2 - 3f_x). \tag{A.3}$$

For either scheme, the expression for PEY $I(\theta)$ is predicted to take the form $I(\theta) = A + B \sin^2\theta$, where A and B are the intercept and slope, respectively, in a NEXAFS intensity versus $\sin^2$ of the incident angle plot such as that shown in Figure 8. If no biaxiality is assumed, the expression for f_x can be given as,

$$f_x = \frac{A + B}{I_{\mathrm{TOT}}} \tag{A.4}$$

where I_{TOT} is the total integrated intensity. Knowing the normalization condition, $f_x + f_y + f_z = 1$ from Stöhr and Samant,[8]

$$I_{\mathrm{TOT}} = \frac{3}{2}(A_{\mathrm{para}} + A_{\mathrm{perp}}) + \frac{3P - 1}{2P}(B_{\mathrm{para}} + B_{\mathrm{perp}}) \tag{A.5}$$

where, P is the polarization of the incident beam, A_{para} and A_{perp} are intercepts A parallel and perpendicular, respectively, to the molecular orientation, and B_{para} and B_{perp} are the slopes B parallel and perpendicular, respectively, to the molecular orientation. In the case of no biaxiality, $A_{\mathrm{para}} = A_{\mathrm{perp}}$ and $B_{\mathrm{perp}} = 0$.

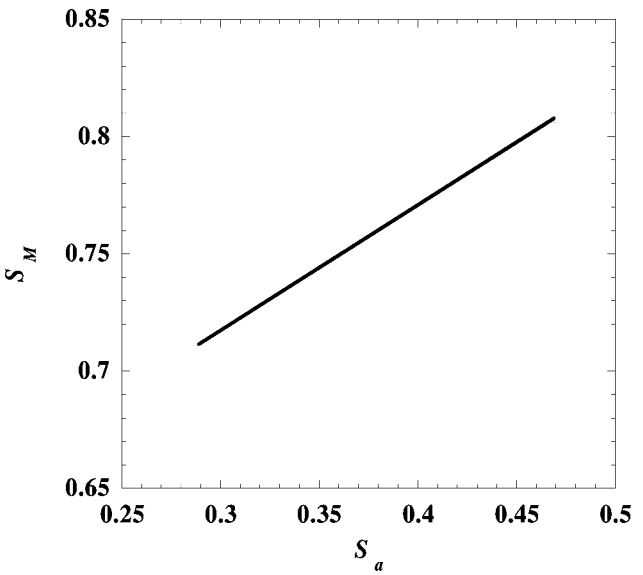

Figure A.1 Plot showing the linear relationship between S_a versus S_M.

Using eqs. (A.4) and (A.5) and substituting the resulting expression for f_x, one arrives to,

$$S_M = \left(1 - \frac{2(A+B)}{A + \frac{B}{6P}(3P-1)}\right) \qquad \text{(A.6)}$$

A plot of the linear relationship between the values of S_a and S_M obtained for the two schemes is shown in Appendix Figure A.1. An important feature of the molecular orientation scheme is that S_M is never less than 0.5, which is consistent with (1) what one might expect from the physical constraint of a semi-rigid molecule confined within a few nm of a surface, and (2) the values of S reported by the use of the surface specific ATR-FTIR by Pirnia and Sung.[6]

References

1. Donald, A. M.; Windle, A. H.; Hanna, S. Liquid Crystalline Polymers; Cambridge University Press: Cambridge, 2006.
2. Onogi, S.; Asada, T. In Reology, Vol. 1; Astarita, G., Marrucci, G., Nicholais, L., Eds.; Plenum: New York, 1980; pp 127–147.
3. Sawyer, L. C.; Jaffe, M. J Mater Sci 1986, 21, 1987.
4. Plummer, C. J. G.; Zulle, B.; Demarmels, A.; Kausch, H.-H. J Appl Polym Sci 1993, 48, 751.
5. Dreher, S.; Seifert, S.; Zachman, H. G.; Moszner, N.; Mercoli, P.; Zanghellini, G. J Appl Polym Sci 1998, 67, 531.
6. Pirnia, A.; Sung, C. S. P. Macromolecules 1988, 21, 2699.
7. Bubeck, R. A.; Thomas, L. S.; Rendon, S.; Burghardt, W. R.; Hexemer, A.; Fischer, D. A. J Appl Polym Sci 2005, 98, 2473.
8. Stöhr, J.; Samant, M. G. J Electron Spectrosc Relat Phenom 1999, 98, 189.
9. Genzer, J.; Kramer, E. J.; Fischer, D. A. J Appl Phys 2002, 92, 7070.
10. Pattison, L. R.; Hexemer, A.; Kramer, E. J.; Krishnan, S.; Petroff, P. M.; Fischer, D. A. Macromolecules 2006, 39, 2225.
11. Bales, S. E.; Hefner, R. E.; Singh, R. U.S. Pat.5,614,599 (1997).
12. Rendon, S.; Burghardt, W. R.; New, A, II; Bubeck, R. A.; Thomas, L. S. Polymer 2004, 45, 5341.
13. Hermans, P. H.; Platzek, P. Kolloid Z 1939, 88, 68.
14. Mitchell, G. R.; Windle, A. H. In Developments in Crystalline Polymers-2; Basset, D. C., Ed.; Elsevier: London, 1988; pp 115–176.
15. Genzer, J.; Sivaniah, E.; Kramer, E. J.; Wang, J.; Xiang, M.; Korner, H.; Char, K.; Ober, C. K.; DeKoven, B. M.; Bubeck, R. A.; Chaudhury, M. K.; Sambasivan, S.; Fischer, D. A. Macromolecules 2000, 33, 1882.
16. Genzer, J.; Sivaniah, E.; Kramer, E. J.; Wang, J.; Xiang, M.; Char, K.; Ober, C. K.; Bubeck, R. A.; Fischer, D. A.; Graupe, M.; Colorado, R.; Shmakova, O. E.; Lee, T. R. Macromolecules 2000, 33, 6068.
17. Genzer, J.; Sivaniah, E.; Kramer, E. J.; Wang, J.; Xiang, M.; Korner, H. M.; Char, K.; Ober, C. K.; DeKoven, B. M.; Bubeck, R. A.; Fischer, D. A.; Sambasivan, S. Langmuir 2000, 16, 1993.
18. Rendon, S.; Burghardt, W. R.; Bubeck, R. A.; Thomas, L. S.; Hart, B. Polymer 2005, 46, 10202.
19. Cinader, D. K.; Burghardt, W. R. J Polym Sci Part B: Polym Phys 1999, 37, 3411.
20. Jung, Y.; Cho, T. Y.; Yoon, D. Y.; Frank, C. W.; Luning, J. Macromolecules 2005, 38, 867.